Nucleation and reshaping thermodynamics of Ni as catalyst of carbon nanotubes

L. H. Liang,[1] F. Liu,[1] D. X. Shi,[1] W. M. Liu,[1] X. C. Xie,[2] and H. J. Gao[1]
[1]*Institute of Physics, Chinese Academy of Sciences, Beijing 100080, China*
[2]*Department of Physics, Oklahoma State University, Stillwater Oklahoma 74078, USA*
(Received 4 March 2005; published 21 July 2005)

A quantitative model describing the nucleation, energy, and diffusion restraints in reshaping of Ni nanoparticles as a catalyst of carbon nanotubes is developed by introducing the size-dependent thermodynamic quantities in the classical nucleation theory and the diffusion laws. The result from our model calculations is in good agreement with that of the latest time-resolved, high-resolution *in situ* transmission electron microscope observation. A new catalytic nanotube growth mechanism is proposed: the growth of a carbon nanotube coupled to the reshaping of the catalyst.

DOI: 10.1103/PhysRevB.72.035453 PACS number(s): 61.46.+w, 64.60.Qb, 66.30.Pa

I. INTRODUCTION

Over the past few years, the study of fabrication and formation mechanisms of carbon nanotubes has attracted great attention due to their intriguing properties and application potential.[1–11] It was found that the original size and mobility of the catalyst can significantly affect the formation and configuration of carbon nanotubes and other kinds of nanotubes or nanowires.[1–11] Various theoretical models of nanotube growth have been suggested,[7–11] and the different approaches, e.g., molecular dynamics[7,10,11] or classic thermodynamics,[8,9] were employed. Two common growth modes are the root growth and the tip growth. In the root or extrusion growth mechanism, the catalyst particles attach to the substrate. The carbon atoms deposit on the catalyst surface and the nanotube stem grows out from the catalyst. The new carbon atoms push the already grown segment upward, i.e., bottom-up growth.[4,5,7,10] The tip-growth mechanism describes the process that the catalysts detach from the substrate, supersaturated carbon atoms separate from the catalyst, and the nanotube grows up-down.[3,4,8,10] However, there are some growth phenomena that do not belong to any of the above two categories,[1,2] thus requiring a new theoretical explanation.

Recently, atomic-scale imaging of carbon nanofiber growth was performed by time-resolved, high-resolution *in situ* transmission electron microscope (hereafter HRTEM) observations.[1] The catalyst Ni particles of approximately 5–20 nm were formed initially, and then the smaller ones elongate from the spherical particles into rods rapidly, with the alignment of graphene sheets on the Ni surface into a multi-layer tubular structure coupled to the reshaping of Ni.[1] When the aspect ratio (length-width) of Ni nanorods reaches to about 4, the elongation ceases and the rods contract abruptly into particles.[1] The elongation and contraction scenarios continue in a periodic manner as the carbon nanotube grows.[1] This detailed knowledge about the growth of carbon nanotubes differs from the root and tip growth mechanism, providing an excellent opportunity for new theoretical study.

In this paper, a model describing the nucleation and reshaping thermodynamics and dynamics of Ni as a catalyst of carbon nanofibers is proposed by introducing the size effect of certain physical quantities within the classic nucleation theory and the diffusion laws. The results from the model calculations are in good agreement with experimental findings. Since the reshaping of the Ni nanoparticle assists the alignment of graphene layers into a tubular structure, the model provides a theoretical background behind the carbon nanotubes formation and might be useful to predict conditions for carbon nanotube formation. More importantly, the model describes a new catalytic nanotube growth mechanism corresponding to the experiments: the carbon nanotube grows coupled to the reshaping of catalyst, different from the known root growth and the tip growth. Note that the growth of carbon nanotubes was studied from the point of view of the catalyst in this work, not focusing on the evolvement detail of the carbon structure itself as in the previous models.[7,8,10,11] The difference of our model from the classic thermodynamic is the introduction of size effect of related physical quantities, and also the model is simple compared to the molecular dynamic method.

II. MODEL AND DISCUSSION

A. Size-dependent nucleation thermodynamics of catalyst Ni particles

First, let us consider the formation of catalyst particles. The total Gibbs free energy change G of the system during the nucleation process includes the volume energy term and the surface/interface energy term,[12]

$$G = -(g/V_s)\pi d^3/6 + \pi d^2 \gamma_{sl}. \quad (1)$$

In the equation above, V_s is the molar volume of the crystal, d is the size of the crystalline nucleus, and γ_{sl} is the solid-liquid interface energy. g denotes the volume Gibbs free energy difference between the crystal and the liquid in the crystallization and is a function of the temperature T with the following form,[13]

$$g = H_m(d) - TS_m(d), \quad (2)$$

in which $H_m(d)$ and $S_m(d)$ are the size-dependent melting enthalpy and entropy, respectively. Note that the thermodynamic equilibrium state is considered here, thus melting enthalpy and entropy are equal to crystallization enthalpy and

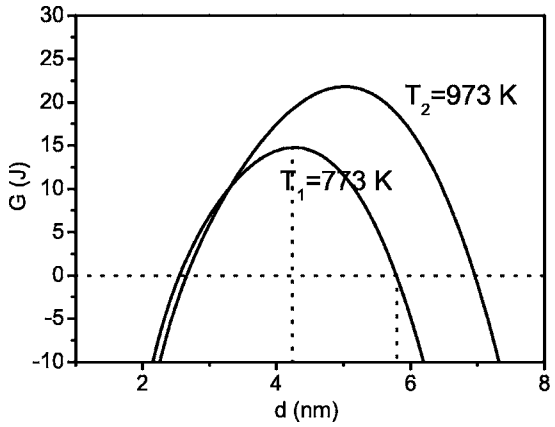

FIG. 1. The size- and temperature-dependent G function in terms of Eq. (1). $H_{mb}=17.47$ KJ mol^{-1} (Ref. 17) in Eq. (3), $S_{mb}=H_{mb}/T_{mb}=10.12$ J mol^{-1} K^{-1} with $T_{mb}=1726$ K.[17] $V_s=6.59$ cm^3 mol^{-1},[17] $h=0.2754$ nm.[18] The dotted lines is an aid to the eye.

entropy, respectively. The only difference from the classical expression is the size dependence in the enthalpy and entropy.

The earlier studies have shown that the melting temperature, melting enthalpy, and melting entropy of nanocrystals decrease as the crystal size d reduces.[14] The size-dependent melting enthalpy $H_m(d)$ is expressed as[14]

$$\frac{H_m(d)}{H_{mb}}=\exp\left(\frac{-2S_{mb}/(3R)}{d/d_0-1}\right)\left(1-\frac{1}{d/d_0-1}\right), \tag{3}$$

where H_{mb} is bulk melting enthalpy and $S_{mb}=H_{mb}/T_{mb}$ is bulk melting entropy with bulk melting temperature T_{mb}. R is the ideal gas constant. d_0 is the critical size at which almost all atoms are at the crystal's surface and is taken as $6h$ for spherical particle with atomic diameter h.[14] The size-dependent melting entropy $S_m(d)$ is given by[14]

$$\frac{S_m(d)}{S_{mb}}=1-\frac{1}{d/d_0-1}. \tag{4}$$

Note that Eqs. (3) and (4) have meaning only when $d>2d_0$.[14] The size of order $2d_0$ represents a length scale characteristic for the crystallinity and is the limit of validity of the model. When $d<2d_0$, the single size effect of thermodynamic quantities may not be sufficient to describe the physical properties of so small-sized particles or clusters.

The size dependence of solid-liquid interface energy γ_{sl} in Eq. (1) has also been considered and is modeled by[15]

$$\gamma_{sl}=\gamma_{slb}(1-d_0/d), \tag{5}$$

where $\gamma_{slb}=2hS_{mb}H_{mb}/(3V_sR)$ is bulk solid-liquid interface energy.[16] Substituting Eqs. (3) and (4) into Eq. (2), and then substituting Eqs. (2) and (5) into Eq. (1), the size-dependent G is obtained.

The maximum of G corresponds to the minimum critical nucleation size. Figure 1 shows that G reaches its maximum at $d=4.2$ nm for $T=773$ K. Thus, the minimum Ni crystal should be larger than 4.2 nm at this temperature, and the stable crystal size is 5.8 nm where $G=0$ and the larger ones correspond to $G<0$. This result agrees with the experimental finding that particles with size of about 5–20 nm were obtained at $T=773$ K.[1] The nucleation size increases with enhancing temperature as shown in Fig. 1, consistent with our general understanding on nucleation. When $T=973$ K, the stable size is about 7 nm and the larger ones corresponds to $G\leqslant 0$, which is also consistent with the experimental proof that the catalyst particles of around 10–30 nm were obtained at this temperature.[2–4] Similarly, the nucleation of iron catalyst follows the same statistical rule.[5,6]

The above energetic consideration can be used to explain the experimentally observed catalystic particle size and its temperature dependence. The formation of catalyst nanoparticles is the first step in carbon nanofibers fabrication and the size of the catalysts affects the diameter of the carbon nanotubes. With carbon atoms deposited on the surface of Ni particles, the particles elongate into nanorods.

B. Reshaping thermodynamics from the Ni nanoparticles to the Ni nanorods

The reshaping is observed at $T=813$ K in the experiment.[1] According to the size-dependent melting temperature model,[14] this temperature reaches about 67% of the melting point of Ni nanocrystals with size 5 nm; the reshaping of Ni particles can proceed kinetically as long as the total free energy decreases in the process.

The total free energy difference ΔG_r between a Ni nanorod and a Ni particle is given by

$$\Delta G_r=V\Delta P+\gamma\Delta S, \tag{6}$$

where ΔP is a pressure difference between the nanorod (P_2) and the particle (P_1), and $V=\pi d_1^3/6=\pi d_2^2L_2/4$ is the volume of the Ni particle and assumed to be constant with d_1 being the diameter of the particle, d_2 and L_2 being the diameter and the length of the nanorod, respectively, and $L_2=2d_1^3/(3d_2^2)$. According to the Laplace-Young equation,[19] $P_1=4f/d_1$ and $P_2=2f/d_2$ where f denotes the intrinsic surface stress of Ni, $\Delta P=2f(1/d_2-2/d_1)$. γ is the surface energy of Ni, ΔS stands for the surface area difference between the nanorod ($S_2=\pi d_2^2/2+\pi d_2L_2$) and the particle ($S_1=\pi d_1^2$), and $\gamma\Delta S=\gamma\pi(d_2^2/2+d_2L_2-d_1^2)$. Let $\eta=d_1/d_2$,

$$\Delta G_r=\pi d_2[2fd_2\eta^2(\eta-2)/3+\gamma d_2(1+4\eta^3/3-2\eta^2)]/2, \tag{7}$$

where the surface stress f is calculated by[15]

$$f=[(9\gamma_{slb}h)/(8\kappa)]^{1/2}. \tag{8}$$

$\kappa=1/B$ is the compressibility of the crystal with volume modulus B. Equation (8) has been used to correctly determine the surface stresses, in agreement with the experimental values.[15] Considering the effect of graphene layers on the surface of Ni, γ in Eq. (7) is the interface energy between Ni and the carbon layer, which is estimated as $\gamma_{sv}/3$,[9] $\gamma_{sv}=2.38$ J m^{-2} (Ref. 20) being the surface energy of free-standing Ni, thus $\gamma=0.793$ J m^{-2}. Note that the surface stress is different from the surface energy, the reversible work per

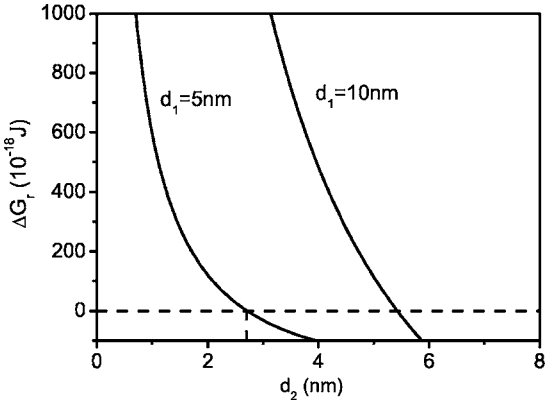

FIG. 2. d_1- and d_2-dependent ΔG_r function in terms of Eq. (7). B=177.3 GPa (Ref. 21) in Eq. (8). The dashed lines are an aid to the eye.

unit area in the plastic deformation process,[19] the stress reflects the reversible work in the elastic deformation,[19] and the influence of carbon shell is not obvious. Equation (7) in fact contains the elastic energy in reshaping through the surface stress.

According to Eq. (7), given d_1, the corresponding minimum d_2 can be obtained by setting ΔG_r=0. When $\Delta G_r < 0$, the Ni nanoparticle transforms its shape spontaneously from the spherical one to a rod. ΔG_r as a function of d_1 and d_2 determined by Eq. (7) is shown in Fig. 2. For example, at d_1=5 nm, d_2=2.7 nm from ΔG_r=0, which agrees with the experimental result that the diameter of the Ni nanorods is about 3 nm.[1]

Let $\xi = L_2/d_2 = 2\eta^3/3$, the length-width ratio of a nanorod. Figure 3 shows the d_1 and d_2 dependences of ξ. At d_2=2.7 nm, correspondingly d_1=5 nm, L_2=11.3 nm, and ξ=4.2 reaches the maximum aspect ratio of the rod. ξ is almost a constant for different d_1 with ΔG_r=0, which is consistent with the experimental result that the aspect ratio of Ni nanorods is about 4.[1] The ratio $\eta = d_1/d_2$ with ΔG_r=0 is also a constant of about 1.8, i.e., the maximum reduction of the diameter of the rods is about half compared to the diameter of the initial particles. Then the rods contract with increasing diameters as the energy continues to decrease as shown in Fig. 2. When d_2 continues to increase up to the size of the initial d_1, the definition of the rod has lost meaning, thus the present model is limited for that case. Although the rods seem to be in a metastable state compared to the spherical or the elliptical shape, they do actually exist,[1,2] at least as an intermediate state. From the thermodynamic point of view, the competition between the volume energy induced by stress and the surface energy through the interaction with carbon atoms causes the reshaping of the catalyst. With the reshaping of the Ni catalyst, carbon fibers form attached to the Ni surface.

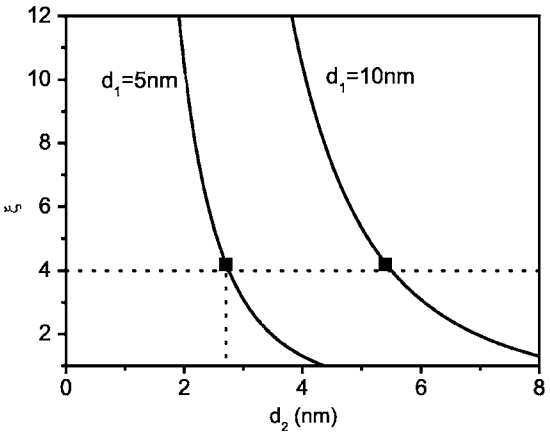

FIG. 3. d_1- and d_2-dependent ξ function, the aspect ratio of the rods. The dotted lines and the symbols are an aid to the eye.

However, the experiment also shows that larger particles may not elongate into rods, but tend to form a pear-like shape.[1,6] Therefore, only the energy consideration mentioned above is not sufficient and an understanding of the particle diffusion process becomes necessary.

C. Diffusion limit of atoms in reshaping of Ni

The experiment shows that the reshaping of Ni occurs in a very short time,[1] related to the rapid diffusion of Ni atoms. Let L be diffusion length at time t, according to Fick's second law,[22]

$$L^2 = Dt. \tag{9}$$

Based on the Arrhenius law, the temperature-dependent diffusion coefficient D is expressed as[23]

$$D = D_0 \exp[-Q/(RT)]. \tag{10}$$

D_0 is a preexponential constant; Q is the activation energy and is proportional to the melting temperature of the materials.[24] Since the melting temperature is size dependent, Q has a similar size dependence as follows,[24]

$$Q = Q_b \exp\left(\frac{-2S_{mb}/(3R)}{d/d_0 - 1}\right), \tag{11}$$

where Q_b is the bulk activation energy. Substituting Eq. (11) into Eq. (10), and then substituting Eq. (10) into Eq. (9), the diffusion length at a given time can be obtained.

Equations (11) and (10) indicate that the diffusive activation energy decreases and the diffusion coefficient increases as the size of the nanocrystals reduces as shown in Fig. 4. Namely, the atom diffusion is easier for smaller particles. The faster migration of atoms in nanocrystals than in bulk may be induced by the increase of the surface/volume ratio where the surface atomic diffusion is faster due to the smaller diffusion energy barrier.[1] A recent study also showed that heat conduction and diffusion in low-dimensional systems may be anomalous.[26]

On the other hand, Fig. 4 shows that the size dependence of the ratio D/D_b, $D_b = D_0 \exp[-Q_b/(RT)]$ being the bulk diffusion coefficient, decreases as the temperature increases although D or D_b itself increases with increasing temperature. This behavior is caused by decreasing of atomic diffusion difference between the nanocrystals and the corresponding bulk crystals with increasing temperature.

For the Ni particle of 5 nm, the activation energy is decreased by 33% compared with the bulk value according to

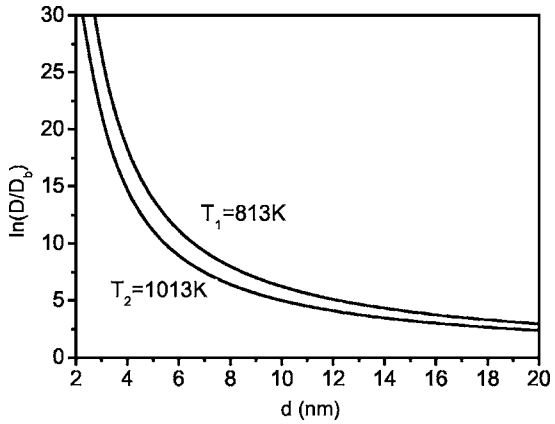

FIG. 4. The size- and temperature-dependent diffusion coefficient $\ln(D/D_b)$ in terms of Eqs. (10) and (11). $Q_b = 284.24$ KJ mol^{-1} (Ref. 25) in Eq. (11). $D_0 = 1.9$ cm^2 s^{-1} (Ref. 25) in Eq. (10).

Eq. (11). This leads to an increase of six orders in the diffusion coefficient according to Eq. (10) at $T = 813$ K, from 10^{-22} to 10^{-16} m^2 s^{-1}, due to the exponential dependence on Q. Therefore, the diffusion length L per second ($t = 1$ s) can reach 10 nm based on Eq. (9), which is consistent with the experimental result[1] and the above prediction of $L_2 = 11.3$ nm based on the energetic consideration.

While for the Ni particle of 20 nm, the activation energy decreases about 7% compared to the bulk value, and the increase of the diffusion coefficient is not apparent (see Fig. 4), D is about 2×10^{-21} m^2 s^{-1}. The diffusion length per second is only about 0.05 nm, which implies the larger particles are not easy to transform into the rods or wires. The above analysis agrees with the experimental results.[1] Our calculations show that the diffusion for particles of 10 nm tends to be difficult, suggesting that the smaller catalyst particles are essential for the formation of longer nanofibers in the coupling growth.

III. CONCLUSIONS

Based on the above discussions, the model describes a novel catalytic nanotube growth mechanism corresponding to the experiments. In this mechanism, the catalyst particles as seeds are formed. The carbon atoms deposit on the catalyst surface and the catalyst particles elongate. The nanotube grows out from the catalyst end and couples to the reshaping and movement of the catalyst. The new atoms pushed the already grown segment forward. This route of growth has been observed by time-resolved HRTEM in Ref. 1 and may also be the fact in some other experiments.

In summary, a quantitative model was developed by introducing the size effect of relevant thermodynamic quantities into the classical nucleation and diffusion theories. The model successfully explains the nucleation and reshaping of catalyst Ni particles and thus provides a thermodynamic basis for the coupling growth of carbon nanotubes. A new nanotube growth mechanism—the growth coupled to the reshaping of catalyst—was proposed.

ACKNOWLEDGMENTS

This work was supported by the NSF of China with Grant Nos. 60276041, 60228005, 10347122, 60490280, 90403034, and 90406017, the China Postdoctoral Science Foundation, and the K. C. Wong Postdoctoral Foundation of the Chinese Academy of Sciences. XCX is supported by US-DOE through DE-FG02-04ER46124. The authors would like to thank B. W. Li for helpful discussions.

[1] S. Helveg, C. Lopez-Cartes, J. Sehested, P. L. Hansen, B. S. Clausen, J. R. Rostrup-Nielson, F. Abild-Pederson, and J. K. Norskov, Nature (London) **427**, 426 (2004).
[2] M. Yudasaka, R. Kikuchi, T. Matsui, Y. Ohki, S. Yoshimura, and E. Ota, Appl. Phys. Lett. **67**, 2477 (1995).
[3] M. H. Kuang, Z. L. Wang, X. D. Bai, J. D. Guo, and E. G. Wang, Appl. Phys. Lett. **76**, 1255 (2000).
[4] V. I. Merkulov, A. V. Melechko, M. A. Guillorn, D. H. Lowndes, and M. L. Simpson, Appl. Phys. Lett. **79**, 2970 (2001).
[5] L. Liu and S. S. Fan, J. Am. Chem. Soc. **123**, 11502 (2001).
[6] C. Klinke, J. M. Bonard, and K. Kern, J. Phys. Chem. B **108**, 11357 (2004); L. Vitali, M. A. Schneider, K. Kern, L. Wirtz, and A. Rubio, Phys. Rev. B **69**, 121414(R) (2004).
[7] A. Maiti, C. J. Brabec, and J. Bernholc, Phys. Rev. B **55**, R6097 (1997).
[8] H. Kanzow and A. Ding, Phys. Rev. B **60**, 11180 (1999).
[9] Q. Jiang, Y. W. Wang, and J. C. Li, Appl. Surf. Sci. **152**, 156 (1999).
[10] S. B. Sinnott, R. Andrews, D. Qian, A. M. Rao, Z. Mao, E. C. Dickey, and F. Derbyshire, Chem. Phys. Lett. **315**, 25 (1999); X. Fan, R. Buczko, A. A. Puretzky, D. B. Geohegan, J. Y. Howe, S. T. Pantelides, and S. J. Pennycook, Phys. Rev. Lett. **90**, 145501 (2003).
[11] Y. H. Lee, S. G. Kim, and D. Tomanek, Phys. Rev. Lett. **78**, 2393 (1997); M. Menon, E. Richter, A. Mavrandonakis, G. Froudakis, and A. N. Andriotis, Phys. Rev. B **69**, 115322 (2004).
[12] D. Turnbull and J. C. Fisher, J. Chem. Phys. **17**, 71 (1949).
[13] D. Turnbull, J. Appl. Phys. **21**, 1022 (1950).
[14] Q. Jiang, H. X. Shi, and M. Zhao, J. Chem. Phys. **111**, 2176 (1999); L. H. Liang, C. M. Shen, S. X. Du, W. M. Liu, X. C. Xie, and H. J. Gao, Phys. Rev. B **70**, 205419 (2004).
[15] Q. Jiang, D. S. Zhao, and M. Zhao, Acta Mater. **49**, 3143 (2001); Q. Jiang, L. H. Liang, and D. S. Zhao, J. Phys. Chem. B **105**, 6275 (2001).
[16] Q. Jiang, H. X. Shi, and M. Zhao, Acta Mater. **47**, 2109 (1999); Z. Wen, M. Zhao, and Q. Jiang, J. Phys. Chem. B **106**, 4266 (2002).
[17] *Periodic Table of the Elements* (Sargent-Welch Scientific Company, Skokie, Illinois, 1980), p. 1.
[18] H. W. King, in *Physical Metallurgy*, edited by R. W. Cahn (North-Holland Publishing Co., Amsterdam, 1983), p. 64.
[19] R. C. Cammarata and K. Sieradzki, Annu. Rev. Mater. Sci. **24**,

215 (1994); J. Weissm1ller and J. W. Cahn, Acta Mater. **45**, 1999 (1997).

[20] L. Vitos, A. V. Ruban, H. L. Skriver, and J. Kollar, Surf. Sci. **411**, 186 (1998).

[21] E. A. Brandes (ed.), *Smithells Metals Reference Book* (Butterworth and Co. Ltd., London, 1983), p. 15-2.

[22] G. E. Murch and A. S. Nowick, *Diffusion in Crystalline Solid*(Academic, Orlando, 1984), p. 6.

[23] K. Dick, T. Dhanasekaran, Z. Y. Zhang, and D. Meise, J. Am. Chem. Soc. **124**, 2312 (2002).

[24] Q. Jiang, S. H. Zhang, and J. C. Li, J. Phys. D **37**, 102 (2004); Q. Jiang, S. H. Zhang, and J. C. Li, Solid State Commun. **581**, 130 (2004).

[25] R. C. Weast, *Handbook of Chemistry and Physics* (Chemical Rubber Co., Cleveland, 1988-1989), p. F-56.

[26] B. W. Li and J. Wang, Phys. Rev. Lett. **91**, 044301 (2003); L. A. Zepeda-Ruiz, J. Rottler, S. Han, G. J. Ackland, R. Car, and D. J. Srolovitz, Phys. Rev. B **70**, 060102(R) (2004).